First-principles study of self- and solute diffusion mechanisms in γ'-Ni_3Al

Priya Gopal* and S. G. Srinivasan†
Department of Materials Science and Engineering, University of North Texas, Denton, USA
(Received 2 April 2012; published 26 July 2012)

Multiple, competing diffusion mechanisms have been postulated in $L1_2$ ordered compounds such as Ni_3Al due to the presence of two distinct sublattices for self- and solute diffusion. They involve intrasublattice, intersublattice, two-pair vacancies, the six-jump cycle, and the antisite assisted jumps. In this work we systematically study these diffusion paths in $L1_2$ ordered Ni_3Al, postulated from three decades of experiments, by coupling density functional theory and the nudged elastic band methods. We determine activation barriers for self-diffusion (Ni and Al) atoms and solute diffusion (Cr, Co, and Ti) atoms, and also explore how solutes influence self-diffusion activation barriers. These calculations reveal that Ni vacancies mediate both self- and solute diffusion in ordered Ni_3Al. Other findings include: (i) Ni atoms diffuse in their own sublattice via nearest neighbor jumps, (ii) Al atoms also preferentially diffuse in the Ni sublattice, (iii) solutes in the proximity of vacancies strongly affect the formation and also the migration energies in problems studied here, and (iv) diffusion mechanism(s) of solutes depend strongly on whether they occupy a Ni or Al site. This site occupancy is predicted by our activation barrier calculations and agrees with experiments. Our calculations reveal that antisite assisted solute diffusion has the lowest activation barrier. However, experiments report a higher activation barrier that correspond to the barriers for the six jump cycle mechanism determined by our calculations. Thus, our calculations together with published experimental work point to multiple, competing mechanisms driving the diffusion of ternary elements in Ni_3Al.

DOI: 10.1103/PhysRevB.86.014112 PACS number(s): 31.15.A−

I. INTRODUCTION

Diffusion is a strong thermally activated process that drives migration of atoms in materials and ultimately governs the evolution of their microstructure and properties. It plays a dominant role at high temperatures where phenomena such as creep and oxidation are accelerated by interdiffusion.[1] For example, controlling diffusion in Ni-based single crystal superalloys through microstructural design leads to their high creep strength at elevated temperatures and makes them suitable for use in turbines for power generation and jet propulsion.

Ni-based superalloys are typically composed of the $L1_2$ ordered γ'-phase of (Ni_3Al) coherently precipitated in a face-centered-cubic (fcc) γ phase Ni matrix. Ni_3Al is the strengthening phase with a Cu_3Au prototype crystal structure with the face-centered sublattice (α) occupied by Ni atoms and the corner sublattice (β) occupied by Al atoms. The creep strength, oxidation resistance, and fatigue tolerance of this base alloy is enhanced by the addition of substitutional solutes such as Co, Cr, Mn, Mo, Os, Re, Ru, Ti, and W. These solute atoms occupy the Ni (α) site, Al (β) site, or both. Some studies reveal a change in the site preference of these alloying additions with changes in temperature and composition,[2,3] which is directly related to the solute diffusion in the ordered phase. Thus, understanding self-diffusion and solute diffusion in model Ni_3Al intermetallic compound is important from a fundamental scientific standpoint and for designing superior Ni-based superalloys.

A large number of experimental[4–8] and theoretical work[9,10] postulate multiple self-diffusion mechanisms in pure Ni_3Al. However experimental understanding of the diffusion of Al atoms is still lacking due to the unavailability of a stable Al isotope. Thus, first-principles calculations can compliment experiments by providing an accurate description of diffusion, especially how each alloying addition influences diffusion mechanisms, in binary systems. For example, Reed *et al.*[11] disproved the conventional view that larger atoms diffuse more slowly in solute doped elemental Ni(fcc) using density functional theory (DFT) methods. More recently Trinkle *et al.*[12] revisited the problem of oxygen diffusivity in α-Ti and discovered new pathways for oxygen diffusion. These results suggest that even simple elemental systems have complex diffusion mechanisms. In comparison, diffusion in $L1_2$ (Ni_3Al) intermetallic structures is much more complicated due to the contribution of both α and β sublattices and by the presence of antistructure defects in addition to vacancies. In the case of solute diffusion in ternary alloys, experimental data is often unavailable and the diffusion processes more diverse.[13] Based on experience, one can conclude that systematic first-principles-based quantitative comparison of the energetics of various diffusion mechanisms for alloying additions in (Ni_3Al) intermetallics can be beneficial. Such a study has not been performed in the literature to the best of our knowledge.

In this work, we use DFT calculations to study the formation energy of point defects and migration pathways responsible for *self-diffusion* of Ni and Al atoms, and *solute diffusion* of Co, Cr, and Ti ternary additions in Ni_3Al. In addition we also report how the solute additions influence Ni and Al migration barriers. We note that dynamics of diffusion can be understood more completely by using kinetic Monte Carlo (kMC) simulations. kMC simulations need a catalog of potential migration pathways and the barrier energies for those pathways. Such a catalog will be provided by our systematic DFT investigation of diffusion mechanisms in binary (Ni_3Al) and ternary (Ni_3Al-X; X = Co,Cr, Ti) alloys. The results of our kMC simulations will be discussed in a forthcoming paper. Note that we focus on Cr, Co, and Ti solutes because they are commonly used in Ni_3Al and are strong partitioning elements in the γ-γ' interface as seen in recent atom probe tomography experiments in RENE-88 superalloy.[14,15] This work showed

that while Ti and Cr prefer the Al sublattice, Co does not have a strong preference for either. The diffusional interaction studies carried out in this manuscript can also help us determine the site preference of these alloying additions.

II. PREVIOUS EXPERIMENTAL AND ' THEORETICAL WORK

In the $L1_2$ Ni_3Al crystal structure, each Ni atom is surrounded by eight nearest neighbor Ni atoms and four Al atoms, while each Al atom is surrounded by 12 Ni atoms. Experiments[4,16] and theoretical calculations[17] indicate that stoichiometric Ni_3Al contains antisite defects and Ni vacancies. The concentration of Ni vacancies is an order of magnitude higher than the Al vacancy concentration, while the concentration of Ni and Al antisites is higher than the Ni vacancy concentration. The diffusion process in Ni_3Al is expected to be mediated by Ni vacancies and antisite defects. The exact mechanisms are unclear. The self-diffusion coefficients of Ni from radio tracer diffusion[4,5,18,19] and interdiffusion experiments[6] are in agreement. Its activation energy estimated by experiments was around 3.03 eV, and the diffusion coefficient (D_{Ni}) is 3.59×10^{-4} m^2/s. The activation energy equals the sum of the formation energy (1.6 eV) and the migration energy (1.2 eV) of a Ni vacancy in Ni_3Al. From these experiments, Ni diffusion in Ni_3Al was inferred to be mediated by the Ni vacancies on the Ni sublattice.

For Al, there are fewer radio-tracer experiments because of the lack of a suitable stable Al radioisotope.[20] However, the Ni-diffusion coefficient from Larikov *et al*. disagrees with accepted literature values. To quantify Al diffusion, other radio tracers like Ge, Ga, Ti, and Nb have been used as probe atoms in impurity diffusion experiments.[19,21] Interdiffusion experiments performed by Ikeda[22] gave an Al self-diffusion coefficient three or four orders of magnitude smaller than the Ni diffusion coefficient. On the contrary, experiments by Fujiwara[23] show that Al and Ni have similar diffusion rates. Clearly there is much discrepancy in the Al-diffusion mechanism(s) given this big dispersion in the diffusion values from radio-tracer experiments.[21,24] In the case of ternary additions, there is even a greater paucity of experimental data. Diffusivities of Cr, Co, and Ti in Ni_3Al have been determined using diffusion couple experiments by Minamino *et al*.[13,21,25] There exist experimental reports on a few other solutes: Mn, Nb, Re, Ru etc.[25–28] However, theoretical understanding of the mechanisms contributing to diffusion is not well studied to the best of our knowledge.

Simulation studies have mostly used kMC[29,30] and molecular dynamics (MD)[10,31–35] employing semiempirical potentials to study formation energies of point defects and self-diffusion in Ni_3Al. A more limited set of first principles calculations[36] investigating self-diffusion mechanisms in Ni_3Al also exist. The MD calculations use Finnis-Sinclair (FS),[37] embedded atom method (EAM),[10,38] and modified EAM[34,39] interatomic potentials. Vitek[31] reported migration barriers for nearest neighbor (NN) jumps for Ni and Al atoms mediated by Ni vacancy. The reported values for migration of a Ni atom is in the range of 0.9–1.4 eV, which is in agreement with the experimental values of $1.2 + / - 0.1$ eV.[4,18] For migration of Al on its own sublattice, there was a discrepancy in the calculated energy barriers: Simulations using EAM[38] reported a value of 1.83 eV, while MEAM[39] and DFT calculations[36] yielded 23.80 eV and 3.36 eV, respectively. For Ni diffusion, only the NN jump barriers were reported. Semiempirical potential calculations of energy barrier for next-nearest-neighbor (NNN) jumps yielded a very high value of 16.59 eV,[34] in disagreement with the DFT value of 3.50 eV.[36]

The experimental and theoretical investigations can be summarized as follows: (1) The activation barrier for Ni atoms to diffuse through the Ni sublattice is lower compared to the other mechanisms and dominates diffusion. (2) The Al atom diffusion mechanism is complex and clear experimental evidence is lacking. Furthermore, there are inconsistencies in the computational results. (3) Semiempirical molecular dynamics calculations using interatomic potentials within EAM and MEAM have been used to obtain migration barriers.[32] Although these potentials describe the nearest neighbor jump in agreement with the experiments and DFT calculations, the barrier for NNN jumps calculated using MEAM is an order of magnitude higher than the DFT derived barrier. (4) The mechanism for solute diffusion has been studied only for a limited number of cases and the minimum energy pathways (MEP) need to be investigated thoroughly.

III. SIMULATION METHODOLOGY

Our first-principles, spin-averaged calculations were carried out using the Vienna *ab initio* simulation package (VASP) employing the projected augmented plane wave (PAW) method.[40,41] Electron exchange and correlation is described within the generalized gradient approximation (GGA) using the Perdew-Burke-Ernzerhof (PBE) parametrization. Since Ni_3Al is metallic, partial occupancies for Brillouin zone integration was accounted for by using the Methfessel-Paxton smearing with a smearing width of 0.2 eV. For a single unit cell, the energy cutoff and the k-point mesh used were 450 eV and $12 \times 12 \times 12$, respectively. The calculated lattice constant a_0 and bulk modulus B were 3.567 Å and 179 GPa respectively, and compared well with the experimental values of 3.57 Å and 174 GPa, respectively.[1] For the defect formation and the migration energy calculations, we constructed a $3a_0 \times 3a_0 \times 3a_0$ supercell containing 108 atoms and used a $3 \times 3 \times 3$ k-point mesh. The convergence threshold for the total energy was 1×10^{-5} eV. For all these calculations, the atoms' positions were relaxed until the forces on each atom were less than 0.005 eV/Å. The diffusion is mediated by vacancies and is quantified by the diffusion constant D that shows an Arrhenius dependence on temperature given by

$$D = D_0 e^{(-Q/K_b T)} = D_0 e^{(-(E_f + E_m)/K_b T)}, \quad (1)$$

where D_0 is the prefactor, and Q is the activation energy for diffusion given by the sum of vacancy formation (E_f) and migration (E_m) energies. The quantity E_m determines the diffusion of the atoms in a material. To calculate E_m, we use the climbing image nudged elastic band method (NEB)[42] implemented in VASP[42] to locate the transition state (TS). Within this formalism, a series of images are constructed by interpolating the atomic positions between the initial and the final states, and connecting them by an elastic band. The band of images is then relaxed until a certain force threshold on the

TABLE I. Point-defect formation energies, (E^f) calculated using Wagner-Schotky formalism are compared with literature. References *a* through *d* are Refs. 44–47, respectively.

Defect	E^f (eV)	Literature
V_{Ni}	1.64	1.15^a, 1.58^b, 1.42^c, 1.47^d
V_{Al}	3.57	3.09^a, 3.64^b, 1.77^c, 2.65^d
Ni_{Al}	1.95	2.04^a, 0.23^c, 0.58^d
Al_{Ni}	−0.84	-0.92^a, -0.97^b, 0.04^c, 0.54^d

images is reached. Once the TS is found, the migration energy barrier is determined from the energy difference between the TS and the initial minimized configuration. We used five images in our NEB computations, and the relaxation threshold for the images was 10^{-2} eV/Å.

IV. RESULTS AND DISCUSSION

Four species of intrinsic point defects likely mediate diffusion in $L1_2$ Ni_3Al. They are vacancies, V_{Ni} and V_{Al}, on the Ni and Al sublattices, respectively, and Al_{Ni} and Ni_{Al} antisite atoms. We first calculate their formation energies using the Wagner-Schottky model[43] before determining migration barriers (energies are shown in Table I). The overall trend of the formation energy agrees with earlier calculations: Vacancy formation energies are higher than antisite formation energies, and V_{Ni} form more easily than V_{Al}.

A. Energy barriers and mechanisms for Ni and Al self-diffusion

In $L1_2$ intermetallic compounds, the major element generally has higher diffusivity. For example, in compounds like Ni_3Ge, Pt_3Mn, and Co_3Ti the diffusivity of α occupiers is orders of magnitude higher than the β occupiers.[48] In Ni_3Al, however, some experiments hint that the above rule might not hold true.[4,19,20] The lack of a suitable stable Al isotope makes the experimental verifications difficult. Hence a systematic investigation of the energetics of various diffusion pathways using DFT can be helpful. In this section, we study one-step and correlated jump mechanisms, including the two-step antistructure bridge (ASB) and six jump cycle (6JC), for Ni and Al atoms in Ni_3Al.

1. Sublattice one-step mechanism

The simplest diffusion mechanism for Ni and Al atoms is the exchange of an atom with a vacancy on its own sublattice. Note that a Ni atom can move on its own sublattice via NN or NNN jumps without creating disorder. For an Al atom, the *intrasublattice* motion involves the NNN jump while the NN jump is an *intersublattice* motion that always introduces disorder in the lattice. A schematic of the sublattice diffusion and the MEP plots for the jumps are shown in Fig. 1. It is clear that the NN jump for Ni is energetically favorable. For the Al atom, the NNN jump mechanism has a higher energy barrier and is less likely. Based on energy consideration, Al atoms will likely diffuse via NN Ni vacancies.

The barrier energies for elementary jumps for Ni and Al presented in Tables II and III agree well with previous semiempirical[32,49] and first-principles calculations.[36] The

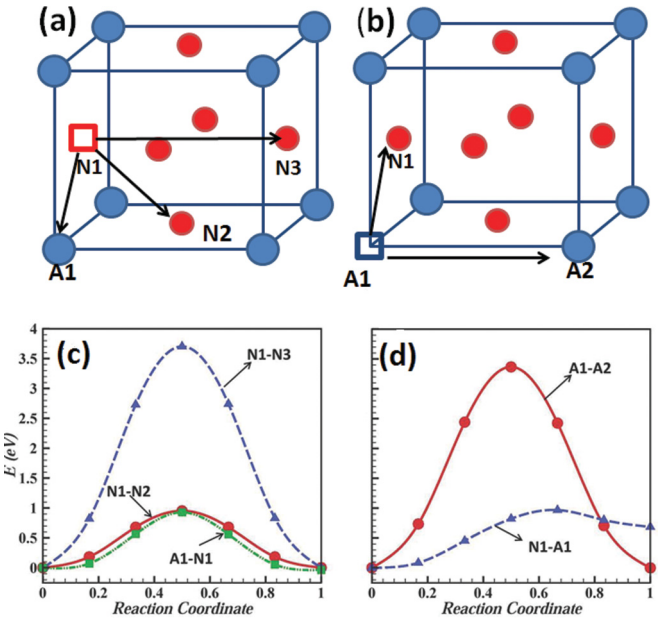

FIG. 1. (Color online) (a) and (b) show diffusion pathways schematically. (c) and (d), respectively, show MEP for Ni and Al sublattice jumps. Here, N1 − N2 = NN intrasublattice jump, N1 − N3 = NNN intrasublattice jump), N1 − A1 = NN intersublattice jump, and A1 − A2 = NNN intrasublattice jump.

barriers for NNN jumps calculated using the semiempirical potentials are higher by an order of magnitude for both Ni and Al atoms.

2. Six-jump cycle mechanism (6JC)

Since the NN jump for Al atoms creates disorder, Young *et al.*[50] proposed the so-called six-jump cycle (6JC) mechanism. As shown in the schematic in Fig. 2, the 6JC consists of a sequence of six NN jumps of Al and a Ni atom. The first three jumps move atoms to the wrong sites creating disorder, while the final three jumps displace atoms to the appropriate sites and restore the order. Both Ni and Al atoms can move via 6JC mechanisms.

The 6JC mechanism has *bent* and *straight* variants, and the sequence of jumps is shown in Fig. 2. In the *straight* variant, the six jumps occur in a (100) plane while the *bent* variant occurs out-of-plane giving rise to two and three dimensional diffusion of atoms, respectively. The MEP for both these 6JC variants

TABLE II. Energy barriers, E_m (eV), for nearest-neighbor (NN) and next-nearest-neighbor (NNN) sublattice jumps for Ni and Al in Ni_3Al. *Ab initio* results from this work deviate significantly from semiempirical potential calculations reported in the literature. References *a* through *d* are Refs. 31, 34, 38, and 39, respectively.

Jump	This work	Literature
Ni → V_{Ni}(NN)	0.98	0.70^a, 1.03^b, 1.45^c
Ni → V_{Ni}(NNN)	3.70	16.60^b
Ni → V_{Al}(NN)	0.97	0.69^d
Al → V_{Al}(NNN)	3.30	1.84^a, 23.80^c
Al → V_{Ni}(NN)	0.96	1.54^d

TABLE III. Calculated migration barriers, E_m in eV, for a different correlated mechanism of Ni and Al atoms in Ni_3Al. Our DFT results are compared with calculations using semiempirical potentials reported in the literature (*a*, Ref. 32).

	Energy E_m	
Jump	This work	Literature
ASB (Ni)	0.94	0.63, 0.84[a]
ASB (Al)	0.85	1.09, 1.14[a]
AS (Al)	0.80	0.69, 0.92[a]
6JC (straight)	1.83	2.23, 1.74[a]
6JC (bent)	2.10	2.70, 2.25[a]

for Al plotted in Fig. 2 show that the energy barrier for the bent cycle is higher than the straight cycle, and, importantly, barriers for 6JC variants are higher compared to a single step cycle mechanism.

3. *Two-step antisite assisted jumps*

The antisite defects form when Al and Ni atoms jump from their sublattice to the other sublattice. They play a major role

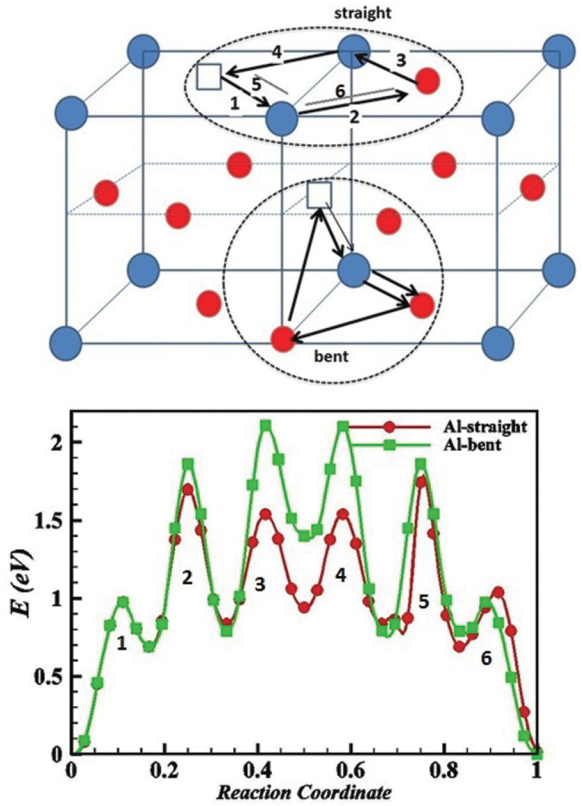

FIG. 2. (Color online) Top: A schematic of the *straight* and *bent* variants of the 6JC mechanism for Ni and Al atoms in Ni_3Al. The nomenclature *straight* refers to the jump sequence in a (100) plane while *bent* refers to an out-of-plane jump sequence. The sequence of six NN jumps are as follows: (1) $V_{Ni} + Al_{Al} \rightarrow V_{Al} + Al_{Ni}$; (2) $V_{Al} + Ni_{Ni} \rightarrow V_{Ni} + Ni_{Al}$; (3) $V_{Ni} + Al_{Al} \rightarrow V_{Al} + Al_{Ni}$; 4) $V_{Al} + Al_{Ni} \rightarrow V_{Ni} + Al_{Al}$; (5) $V_{Ni} + Ni_{Al} \rightarrow V_{Al} + Ni_{Ni}$; (6) $V_{Al} + Al_{Ni} \rightarrow V_{Ni} + Al_{Al}$. Bottom: Minimum energy paths for the straight and bent cases 6JC in Ni_3Al.

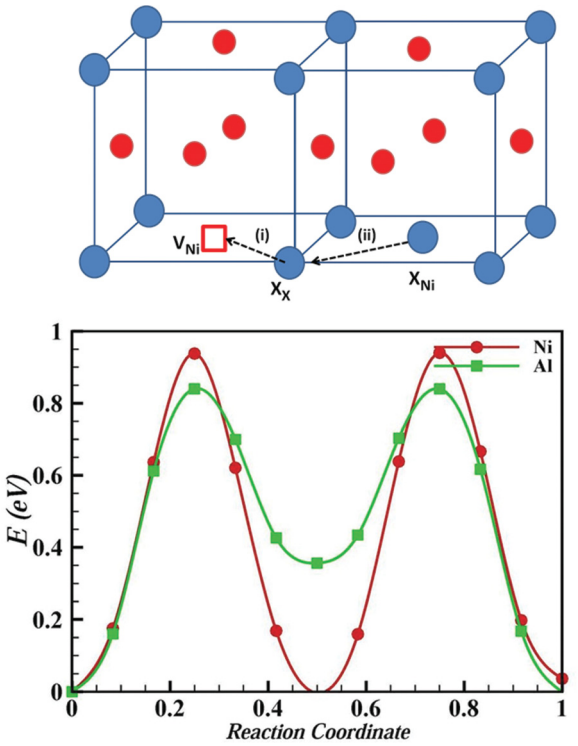

FIG. 3. (Color online) Top: A schematic of atomic arrangements during the ASB mechanism for Ni and Al atoms in Ni_3Al is shown. For Al, V_{Ni} first exchanges with the Al_{Al}. In the second step, V_{Ni} exchanges with the antisite atom Al_{Ni}. The vacancy/atom thus jumps by a lattice constant. Analogous path exists for Ni atoms. Bottom: MEP for ASB mechanism for Ni and Al atoms. The barrier is lower for Al compared to Ni atoms and the potential well is shallower for Al compared to Ni.

in diffusion processes in $L1_2$ ordered compounds, especially at increasing concentration and at higher temperatures. Table I shows that Al antisites form more easily compared to both Ni and Al vacancies and Ni antisites.

Antisite assisted mechanism can occur either via simple NN jumps for Al atoms, or via the so-called antisite bridge mechanism (ASB)[21] for both Ni and Al atoms. In the ASB mechanism for Ni atoms, the Ni_{Al} is a NN to V_{Ni} as shown in the top part of Fig. 3. V_{Ni} first exchanges with Ni_{Al} and then with a regular atom on the Ni sublattice. Thus two Ni atoms are displaced at the completion of this jump. The ASB mechanism for Al atom diffusion involves the exchange of a Ni vacancy with an Al atom on the Al sublattice, and then with an Al antisite (Al_{Ni}). This displaces two Al atoms upon completion. The plots in Fig. 3 show that the energy barrier for the ASB mechanism for Ni and Al atoms are 0.94 eV and 0.85 eV, respectively.

The Al atoms can also diffuse via another antisite assisted mechanism called the antistructure (AS) sublattice mechanism involving simple NN jumps on the Ni sublattice. In this the Al_{Ni} antisite defect diffuses on the Ni sublattice via a NN V_{Ni}. The corresponding migration barrier for this jump, given in Fig. 3, is much lower than other candidate mechanisms for Al diffusion. However, Al_{Ni} and V_{Ni} must occupy the NN position for this jump to occur. This restriction will likely result in a lower mobility of the Al atoms compared to Ni

TABLE IV. Calculated vacancy formation energy (E_v^f) in the presence of Co, Cr, and Ti solutes at Ni and Al sites in Ni_3Al.

	E_v^f (eV)						
Defect	No X	Cr_{Ni}	Co_{Ni}	Ti_{Ni}	Cr_{Al}	Co_{Al}	Ti_{Al}
V_{Ni}	1.64	2.04	0.92	1.67	1.75	1.72	1.90
V_{Al}	3.66	4.25	2.89	3.09	3.68	3.71	3.89

atoms. However, some experimental results[21,25,51] indicate that the ratio of diffusivity of Al atoms is higher than Ni atoms at higher temperatures. In such a case, the ASB mechanism will be more effective.

Our calculations (See Table III) indicate that both the AS and ASB mechanisms have lower energies compared to other mechanisms considered by us and will likely be dominant for Al atoms in pure Ni_3Al. For Ni atoms, the lower migration barrier for NN jumps seen in our calculations agree with previous experimental and theoretical work.[9,10,21,36,45,52] The ASB mechanism for Ni atoms will be more effective when the concentration of Ni_{Al} becomes significant like in Ni-rich alloys.

B. Effect of Co, Cr, and Ti solutes on Ni and Al atom self-diffusion

Solute atoms significantly influence *self-diffusion* kinetics and impact the overall performance of Ni-based superalloys. For example studies of Carter *et al.* on the effect of Pt in B2-NiAl[53] showed that Pt enhanced the diffusivity of Al and Ni atoms. However, the effect of common alloying additions on Ni and Al self-diffusion mechanisms in Ni_3Al are still unclear. In this section we use the approach of Carter to study how Co, Cr, and Ti solutes influence self-diffusion in Ni_3Al. It is known that a solute X, placed in the vicinity of defects/defect clusters, can influence the ease of forming Ni and Al vacancies and antisites in Ni_3Al. Therefore, we will first study solute effects on point-defect formation energies. In principle, there are numerous positions to place the ternary solute, but we restrict ourselves to the NN positions of a defect site. The defect formation energy in the presence of a ternary addition X (X = Cr, Ti, Co) is calculated using the Wagner-Schottky model.[43,54] For the $3 \times 3 \times 3$ supercell, the vacancy formation energy in binary Ni_3Al is given by

$$V_{Ni} = E(Ni_{80}Al_{27}) - E(Ni_{81}Al_{27}) + E(Ni). \quad (2)$$

In the presence of solute X at the Al site, the vacancy formation energy is given by

$$V_{Ni}(X\text{atAl}) = E(Ni_{80}Al_{26}X) - E(Ni_{80}Al_{26}) - E(X). \quad (3)$$

$E(X)$ is the energy of the reference state of solute X. While the reference state is body-centered-cubic (bcc) for Cr, we use the hexagonal-close-packed (hcp) reference structure for Co and Ti. Analogous equations can be written for Al vacancy.

Tables IV and V summarize the influence of ternary Co, Cr, and Ti solutes on formation energies of vacancies at Ni and Al sites in Ni_3Al. We see that the formation energy vacancies decreases significantly when Co is substituted at the Ni sublattice. Thus, it is easier to form vacancies around the Co solutes. On the contrary, both Cr and Ti inhibit the vacancy formation with Ti having a stronger effect. A similar effect is also seen for the migration barriers. The MEP plots are shown in Figure 4 and the barrier energies are summarized in Table V. While Cr and Co decrease the barrier, Ti increases the barrier for Ni-sublattice jumps. However, these solutes have negligible influence on the energetics of the ASB mechanism (see Figs. 4 and 5). But the depth of the energy barriers are affected as seen by shallower energy wells for Ti and Al compared to Cr and Co.

TABLE V. Migration barrier (E_m) for Ni and Al atom jumps when solute atoms are present at Ni and Al sites. Barriers are lower in the presence of Co and Cr atoms, and higher when Ti atoms are present.

	E_m (eV)						
Jump	No X	Cr_{Ni}	Co_{Ni}	Ti_{Ni}	Cr_{Al}	Co_{Al}	Ti_{Al}
Ni $\rightarrow$ V_{Ni}	0.95	0.793	0.892	1.006	0.793	0.86	1.104
Al $\rightarrow$ V_{Al}	3.36	3.95	3.34	4.37	3.33	3.23	3.493
Al $\rightarrow$ V_{Ni}	0.96	1.075	0.937	1.461	0.90	0.858	1.05

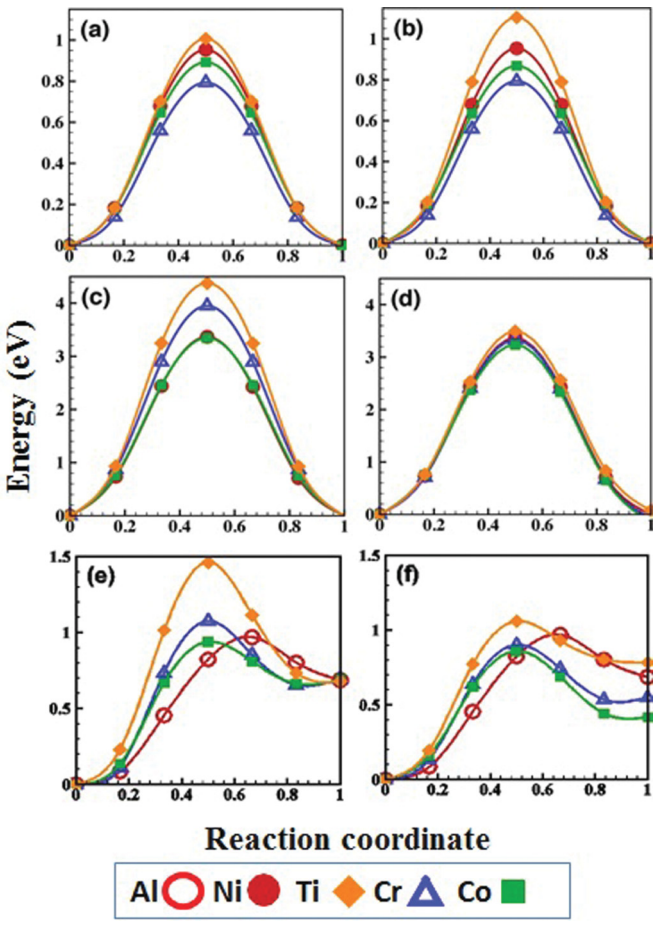

FIG. 4. (Color online) MEP for sublattice one-step jumps for Ni and Al atoms in solute doped Ni_3Al. In (a), (c), and (e), the solute atom was placed at Ni sites. In (b), (d), and (f), solutes were placed at the Al sites. The different migration pathways are as follows: Ni$\rightarrow$$V_{Ni}$ [(a) and (b)], Al$\rightarrow$$V_{Al}$ [(c) and (d)], Al$\rightarrow$$V_{Ni}$ [(e) and (f)].

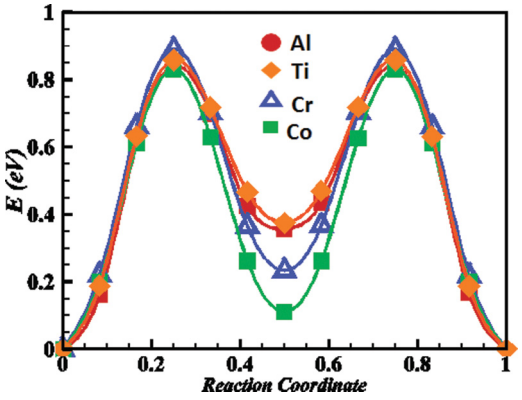

FIG. 5. (Color online) Minimum energy paths for Al diffusion via ASB mechanism in pure and solute doped Ni_3Al systems. Red, blue, green, and orange lines represent no-solute, Cr, Co, and Ti, respectively. Solutes have negligible effect on the migration energy barriers. The potential well is shallower for Co and Cr but remains unchanged for Ti.

C. Co, Cr, and Ti solute atom diffusion

The third piece of the diffusion puzzle in Ni_3Al is the energetics of solute-atom interactions and diffusion, and the attendant site preferences. Impurity diffusion in Ni_3Al-X ternary alloys (X = Pt, Ti, Cr, Fe, Nb, Ga, Mo) have been studied using interdiffusion experiments.[13,21,25–27,45] However, relevant computational studies are still limited.[36,45] For example, Zhang and Wang[36] determined the migration barriers for Re via the NN jump mechanism using the NEB method. Gong *et al.*[45] studied the diffusion of transition metal solutes including Cr, Co, and Ti in Ni_3Al via vacancy drag together with a DFT method.[55] It is important to note that they *assumed* that Al-subsituting elements diffuse as antistructure defects in Ni_3Al. This ignores numerous other postulated diffusion mechanisms and could explain why their activation energies Q for Cr, Co, and Ti diffusion are higher than the corresponding experimental values by 0.5, 0.85, and 2.15 eV.[13]

In this paper, we first determine whether Co, Cr, and Ti solutes prefer the Ni or the Al sublattice sites. Next, we determine the MEP for various postulated diffusion mechanisms that take these solutes out of the Ni_3Al sites they can occupy. We use the NEB method in our calculations.

1. Site preference for Cr, Co, and Ti solutes

The site preference of ternary alloying additions has been reported by a number of researchers using first principles methods.[2,44,56,57] We follow the method introduced by Ruban and Skriver[2] to calculate the site occupancy of ternary alloying additions in Ni_3Al. In this formalism, the site preference is determined by calculating the energetics of the reaction: $X_{Ni} + Al_{Al} \rightarrow X_{Al} + Al_{Ni}$. The energy change term ($\Delta E_X^{Ni\rightarrow Al}$) determines the site preference and is given by

$$\Delta E_X^{Ni\rightarrow Al} = E(Ni_{81}Al_{26}X) + E(Ni_{80}Al_{27}Al) - E(Ni_{80}XAl_{27}) - E(Ni_{81}Al_{27}).$$

Here, $E(Ni_{81}Al_{26}X)$, $E(Ni_{80}Al_{27}Al)$, $E(Ni_{80}XAl_{27})$, and $E(Ni_{81}Al_{27})$ are the total energies of the supercell with X at an Al site, Al at an antisite, X at a Ni site, and pure Ni_3Al, respectively. If ($\Delta E_X^{Ni\rightarrow Al}$) < 0, then X atoms occupy Al sites. On the other hand, X atoms occupy Ni sites if $\Delta E_X^{Ni\rightarrow Al} > (E_{Al_{Ni}} + E_{Ni_{Al}})$. Site occupancy of X is composition dependent when $\Delta E_X^{Ni\rightarrow Al}$ lies in between the above two limits. Note that $E_{Al_{Ni}}$ and $E_{Ni_{Al}}$ are, respectively, the formation energies of the Al and Ni antisites. Table VI gives $\Delta E_X^{Ni\rightarrow Al}$ for Co, Cr, and Ti solutes considered in our study.

TABLE VI. $\Delta E_X^{Ni\rightarrow Al}$ values for solutes and their site preference are given and compared with literature. References *a* and *b* are Refs. 44 and 56, respectively.

Solutes	$\Delta E_X^{Ni\rightarrow Al}$ This work	$\Delta E_X^{Ni\rightarrow Al}$ Literature	Site preference
Cr	−0.92	-0.50^a, -0.10^b	Al
Co	1.04	1.25^b	Composition-dependant
Ti	−0.4	-0.62^b	Al

Additional insight into the site preference is provided by calculating the migration barriers for the $X_{Al} \rightarrow V_{Ni}$ intersublattice jumps. Figure 6 shows the MEP for this jump. Note that this jump is also one of the mechanisms for the solute diffusion. From these plots we see that the barrier energies for Cr, Co, and Ti are higher than that for Al. Importantly, the final configuration wherein a solute atom is at the Ni site is metastable and has a higher energy than the initial state where the solute is at an Al site. This energy is higher by 1.29 and 1.32 eV, respectively, for Cr and Ti and suggests that Cr and Ti prefer the Al site in Ni_3Al. The final state energy for Co is only 0.2 eV higher indicating that it can occupy either Al or Ni sites, with a slight preference for the Al sublattice. Our results agree with previous reports of Cr and Ti preference for Al-sublattice sites while the site preference of Co is composition dependent.[2,44,57]

2. Diffusion mechanisms for Cr, Co, and Ti solutes

From the site preference data it is inferred that the migration paths for Cr and Ti will be similar to that of the Al atoms, while the path(s) for Co is unclear. We first investigate the diffusion of solutes via the one-step NNN jump on the Al sublattice and the 6JC path as shown in Fig. 7. We see that the energies for the Al NNN jumps and 6JC are higher for all three

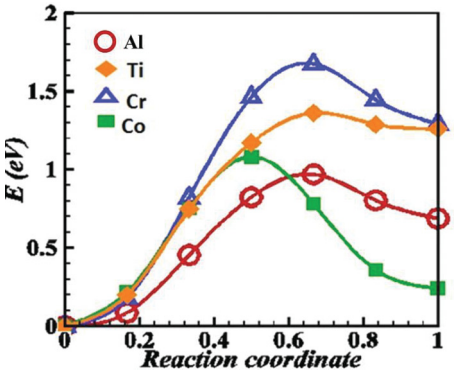

FIG. 6. (Color online) MEP for $X_{Al} \rightarrow V_{Ni}$ jump for solutes in Ni_3Al. Final state energies are higher for all solutes. Co and Al migration barriers are lower than Cr and Ti.

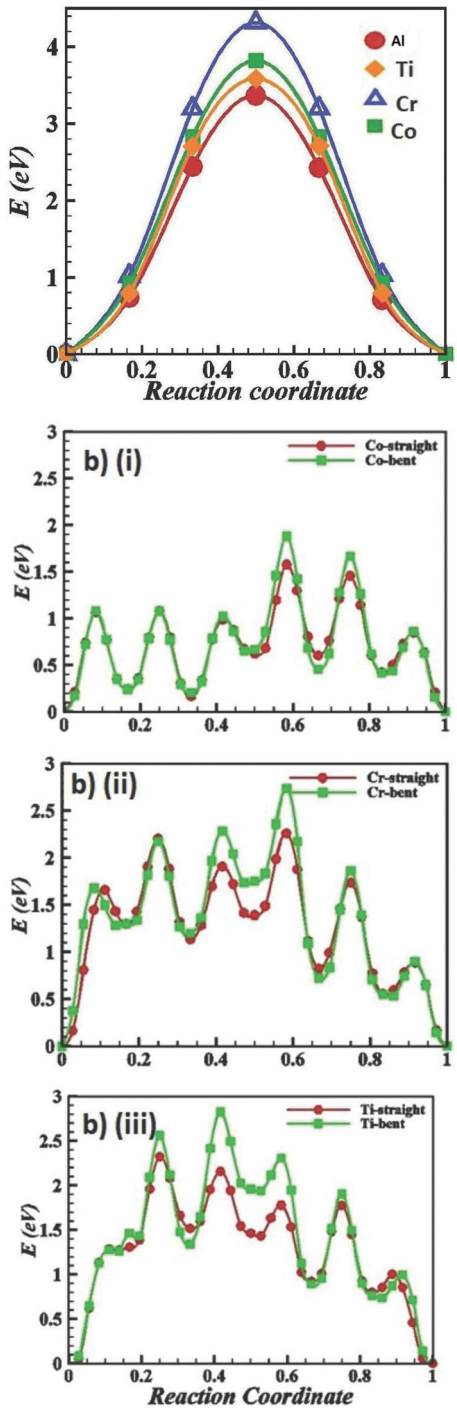

FIG. 7. (Color online) MEP for (a) $X_{Al} \rightarrow V_{Al}$ jump for Cr, Co, and Ti and (b) 6JC mechanism for (i) Cr, (ii) Co, and (iii) Ti.

solutes considered here. The energy barriers are tabulated in Table VII.

As mentioned earlier, antisite assisted AS and ASB mechanisms have been proposed for Al diffusion in Ni_3Al. Divinski *et al*. have argued that these mechanisms also mediate diffusion of Al-substituting solutes.[21] Two possible antisite assisted mechanisms are (i) the Al-substituting elements occupy the Ni sublattice and diffuse as AS defects via NN Ni vacancies and/or (ii) the ASB mechanism via X_{Ni} and V_{Ni} species at NNN positions. Here, the vacancy first exchanges with a

TABLE VII. Calculated migration barriers, E^m in eV, for various solute jumps in Ni_3Al.

Jump	Solute	This work
$X_{Al} \rightarrow V_{Al}$ (NNN)	Cr	4.30
	Ti	3.50
	Co	3.70
$X_{Al} \rightarrow V_{Ni}$	Cr	1.70
	Ti	1.36
	Co	1.08
6JC straight	Cr	2.45
	Ti	2.30
	Co	1.60
6JC bent	Cr	2.83
	Ti	3.40
	Co	1.80
Antisite assisted		
$X_{Ni} \rightarrow V_{Ni}$	Cr	0.70
	Ti	0.29
	Co	0.92
ASB	Cr	1.01
	Ti	0.80
	Co	1.70

regular Al atom and then with the antisite solute X_{Ni}. The MEP plots for AS and ASB mechanisms for Co, Cr, and Ti diffusion in Ni_3Al shown in Fig. 8 reveal that their energy barriers are significantly lower than those for sublattice and 6JC mechanisms. This validates the argument of Divinski *et al*. that antisite defects mediate the diffusion of both Al and solutes occupying the Al site in Ni_3Al.

The activation barriers have been measured for some solutes in Ni_3Al using radio-tracer and interdiffusion experiments.[13,21,27] These values for Co, Cr, and Ti are 3.37, 3.8, and 4.4 eV, respectively. These high energy barriers point to a mechanism more complicated than the simple AS defect

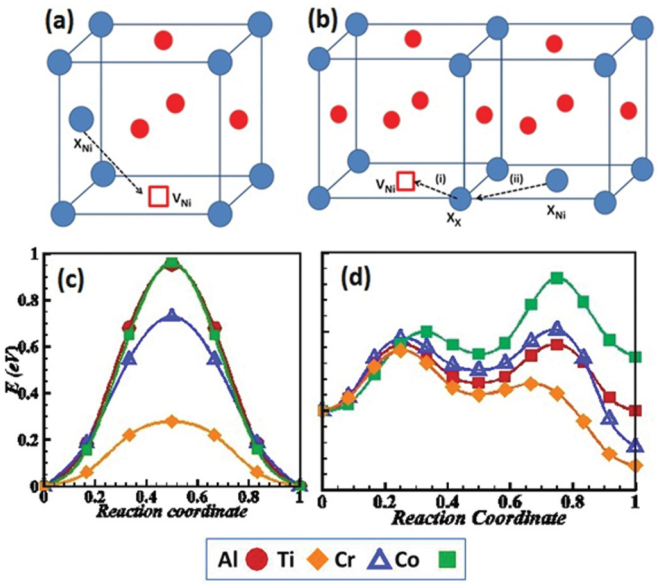

FIG. 8. (Color online) MEP for diffusion of Cr, Co, and Ti solutes in Ni_3Al are shown. (a) $X_{Ni} \rightarrow V_{Ni}$ and (b) two-step ASB mechanism.

$\alpha\alpha$ jump for solutes considered by Gong *et al*.[45] They obtained Q of 2.58, 3.31, and 2.25 eV for Co, Cr, and Ti, respectively. These values differ by more than 0.4 eV from the experimental values. This discrepancy can arise by not considering favorable alternative diffusion mechanisms. Our calculations agree with Gong *et al*.[45] for the AS sublattice mechanism. Nevertheless, we cannot conclusively rule out the migration of Ti via a simple $\alpha-\alpha$ jump as the calculated barrier is 0.29 eV. Also, it is possible that anharmonic lattice vibrations or the correlation effects might play a non-negligible role in Ti diffusion.

We find that the activation energy Q for Co, Cr, and Ti close to experimental values can be obtained if we consider other candidate diffusion mechanisms such as 6JC. For Cr, Q (6JC-straight) is 3.94 eV compared to the experimental value of 3.8 eV. For Ti, our calculations predict the Q (6JC-straight) of 4.20 eV compared to the experimental value of 4.4 eV. For Co, we find that the 6JC mechanism gives a value of 3.24 eV compared to 3.37 eV experimental value.

We have obtained Q values closer to experiments than Gong *et al*. by considering other diffusion mechanisms. While our calculations suggest that the NN diffusion mechanisms will likely be dominant given their lower energy barrier, a comparison with diffusion activation energy determined from experiments suggests the opposite. Therefore, our results reveal that solute diffusion in Ni_3Al is a complex, multi-mechanism driven process given the relatively close values of the energy barriers for the various candidate mechanisms. To understand the synergy between the various mechanisms investigated here it is necessary to carry out KMC simulations of diffusion using energy barriers calculated here. The KMC simulations, providing a comprehensive picture of diffusion by calculating the probability of each mechanism, are part of a forthcoming paper.

V. SUMMARY

We used DFT calculations with the CI-NEB method to study the vacancy-mediated diffusion mechanisms in pure and solute-doped Ni_3Al. The Cr and Ti atoms preferentially occupy the Al sublattice, while Co may occupy Ni or Al sites. The diffusion of Al and Ni atoms occur via Ni sublattice. The migration barriers for Ni and Al atom nearest neighbor jumps are significantly affected by the presence of nearby solute atoms. Co and Cr decrease the energy barriers while Ti increases them. For Al, the calculated barriers indicate that ASB mechanism is favored over the 6JC mechanism. Analysis of the migration paths for Cr, Co, and Ti in Ni_3Al reveal that the energy barriers for solutes is lower in the antisite assisted (AS) mechanism. However our calculated values of the activation barriers for solutes in the 6JC mechanism is in better agreement with the experimental values suggesting that more than one mechanism can contribute to solute diffusion in Ni_3Al.

ACKNOWLEDGMENTS

The US Air Force Research Laboratory funded this work (J. Tiley). We would like to thank Rajarshi Banerjee and Michael I. Baskes for useful discussions. The Talon Linux cluster at UNT and computers at the Texas Advanced Computing Center in Austin funded by NSF were used.

*priya.gopal@unt.edu
†srinivasan.srivilliputhur@unt.edu

[1] M. Donachie and S. Donachie, *Superalloys: A technical guide* (ASM International, Ohio, USA, 2002).
[2] A. V. Ruban and H. L. Skriver, Phys. Rev. B **55**, 856 (1997).
[3] M. Sluiter and Y. Kawazoe, Phys. Rev. B **51**, 4062 (1995).
[4] S. Frank, U. Sodervall, and C. Herzig, Phys. Status Solidi B **191**, 45 (1995).
[5] G. F. Hancock, Phys. Status Solidi A **7**, 535 (1971).
[6] T. Ikeda, A. Almazouzi, M. K. H. Numakura, W. Sprengel, and H. Nakajima, Act. Mat. **46**, 5369 (1997).
[7] Y. Shi, G. Frohberg, and H. Weaver, Phys. Status Solidi A **152**, 361 (1995).
[8] T. M. Wang, M. Shimotomai, and M. Doyama, J. Phys. F **14**, 37 (1984).
[9] G. E. Murch and I. V. Belova, Mater. Res. Soc. Symp. Proc. **527**, 135 (1998).
[10] S. B. Debiaggi, P. M. Decorte, and A. M. Monti, Phys. Status Solidi B **195**, 37 (1996).
[11] A. Janotti, M. Kremar, C. Fu, and R. Reed, Phys. Rev. Lett. **92**, 085901 (2004).
[12] H. H. Wu and D. R. Trinkle, Phys. Rev. Lett. **107**, 045504 (2011).
[13] Y. Minamino, S. Jung, T. Yamane, and K. Hirao, Metall. Trans. A **23**, 2783 (1992).
[14] R. Srinivasan, R. Banerjee, J. Y. Hwang, G. B. Viswanathan, J. Tiley, D. M. Dimiduk, and H. L. Fraser, Phys. Rev. Lett. **102**, 086101 (2009).
[15] J. Tiley, G. B. Viswanathan, R. Srinivasan, R. Banerjee, D. M. Dimiduk, and H. L. Fraser, Acta Mater. **57**, 2538 (2009).
[16] K. Badura-Gergen and H. E. Schaefer, Phys. Rev. B **56**, 3032 (1997).
[17] J. Sun and D. Lin, Acta Metall. Mater. **42**, 195 (1994).
[18] K. Hoshino, S. J. Rothman, and R. S. Averback, Acta Metall. **36**, 1271 (1988).
[19] Y. Shi, G. Frohberg, and H. Wever, Phys. Status Solidi A **152**, 361 (1995).
[20] L. Larikov, V. Geichenko, and V. Falchenko, *Diffusion processes in ordered alloys* (Amerind, Oxonian Press, New Delhi, 1981).
[21] S. V. Divinski, S. Frank, U. Sdervall, and C. Herzig, Acta Mater. **46**, 12 (1998).
[22] T. Ikeda, H. Numakura, and M. Koiwa, Acta Mater. **46**, 6605 (1998).
[23] K. Fujiwara and Z. Horita, Acta Metall. **50**, 1571 (2002).
[24] H. Yasuda, T. Takasugi, and M. Koiwa, Acta. Metall. Mater. **40**, 381 (1992).
[25] Y. Minamino, Y. Yoshida, S. B. Jung, K. Hirao, and T. Yamane, DDF **143**, 257 (1997).
[26] N. Garimella, H. J. Choi, and Y. H. Sohn, Defect Diffus. Forum **297**, 1322 (2008).

[27]E. Mabruri, S. Sakurai, Y. Murata, T. Koyama, and M. Morinaga, Mater. Trans. **49**, 1441 (2008).
[28]H. Numakura, T. Ikeda, M. Koiwa, and A. Almazouzi, Philos. Mag. A **77**, 887 (1998).
[29]G. E. Murch and I. V. Belova, Philos. Mag. A **80**, 1481 (2000).
[30]M. Athenes, P. Bellon, Defect Diffus. Forum **194–199**, 441 (2001).
[31]H. Shenyang, W. Tianmin, and L. Yulan, Modell. Simul. Mater. Sci. Eng. **4**, 493 (1996).
[32]J. Duan, J. Phys.: Condens. Matter **18**, 1381 (2006).
[33]J. Duan, J. Phys.: Condens. Matter **20**, 195221 (2008).
[34]G. X. Chen, D. D. Wang, J. M. Zhang, H. P. Huo, and K. Xu., Physica B **403**, 118 (2008).
[35]Y. Mishin, Acta Mater. **52**, 1451 (2004).
[36]X. Zhang and C.-Y. Wang, Acta Mater. **57**, 224 (2009).
[37]J. Duan, J. Phys.: Condens. Matter **19**, 086217 (2007).
[38]S. Yu, C. Y. Wang, T. Yu, and J. Cai., Physica B **396**, 138 (2007).
[39]J. M. Zhang, H. Yu, K. Xu, and V. Ji, Superlattices Microstruct. **44**, 259 (2008).
[40]G. Kresse and J. Hafner, Phys. Rev. B **47**, 558 (1993).
[41]G. Kresse and J. Hafner, Phys. Rev. B **49**, 14251 (1994).
[42]G. Henkelman, B. P. Uberuaga, and H. Jònsson, J. Chem. Phys. **113**, 9901 (2000).
[43]K. A. Marino and E. A. Carter, Act. Mater. **56**, 3502 (2008).
[44]C. Jiang, D. J. Sordelet, and B. Gleeson, Acta Mater. **54**, 1147 (2006).
[45]X. F. Gong, G. X. Yang, Y. H. Fu, C. Ming, Y. Q. Xi, J. Zhuang, and X.-J. Ning, Comput. Mat. Sci. **47**, 232 (2009).
[46]S. Xiaolin, H. Wangyu, D. Huiqiu, Z. Ying, D. Shengua, W. Chongyu, and Z. Bangwei, Mat. Sci. Forum **475**, 3091 (2005).
[47]A. Caro, M. Victoria, and R. S. Averback, J. Mater. Res. **51**, 409 (1990).
[48]H. Mehrer, Mater. Trans., JIM **37**, 1259 (1996).
[49]S. C. Bocquet, J. Mater. Res. Soc. Symp. Proc. **527**, 165 (1998).
[50]W. M. Young and E. Elcock, Proc. Phys. Soc. **89**, 735 (1966).
[51]T. Ikeda, A. A, H. Namakura, H. Koiwa, W. Sprengel, and H. Nakajima, Defect Diffus. Forum **143–147**, 275 (1997).
[52]H. Numakura, T. Ikeda, H. Nakajima, and M. Koiwa, Mat. Sci. Eng. A **312**, 109 (2001).
[53]K. A. Marino and E. A. Carter, Chem. Phys. Chem. **10**, 226 (2009).
[54]C. Wagner and W. Schottky, Z. Phys. Chem. B **11**, 163 (1931).
[55]X. F. Gong *et al*. (private communication).
[56]Q. Wu and S. Li, Comput. Mater. Sci. **53**, 436 (2012).
[57]M. Chaudhari, A. Singh, P. Gopal, S. Nag, R. Banerjee, and J. Du, Phil. Mag. Lett.1 (2012).